Neurobiology of Disease

# Lymphotoxin β Receptor (LtβR): Dual Roles in Demyelination and Remyelination and Successful Therapeutic Intervention Using LtβR–Ig Protein

**Sheila R. Plant,[1,2]* Heather A. Iocca,[1]* Ying Wang,[1] J. Cameron Thrash,[4] Brian P. O'Connor,[1] Heather A. Arnett,[1,2] Yang-Xin Fu,[5] Monica J. Carson,[4] and Jenny P.-Y. Ting[1,2,3]**

[1]Lineberger Comprehensive Cancer Center, [2]Neuroscience Center, and [3]Department of Microbiology-Immunology, University of North Carolina, Chapel Hill, North Carolina 27599, [4]Division of Biomedical Sciences, University of California, Riverside, California 92521, and [5]Department of Pathology, The University of Chicago, Chicago, Illinois 60637

**Inflammation mediated by macrophages is increasingly found to play a central role in diseases and disorders that affect a myriad of organs, prominent among these are diseases of the CNS. The neurotoxicant-induced, cuprizone model of demyelination is ideally suited for the analysis of inflammatory events. Demyelination on exposure to cuprizone is accompanied by predictable microglial activation and astrogliosis, and, after cuprizone withdrawal, this activation reproducibly diminishes during remyelination. This study demonstrates enhanced expression of lymphotoxin β receptor (LtβR) during the demyelination phase of this model, and LtβR is found in areas enriched with microglial and astroglial cells. Deletion of the LtβR gene (*Ltβ*$R^{-/-}$) resulted in a significant delay in demyelination but also a slight delay in remyelination. Inhibition of LtβR signaling by an LtβR–Ig fusion decoy protein successfully delayed demyelination in wild-type mice. Unexpectedly, this LtβR–Ig decoy protein dramatically accelerated the rate of remyelination, even after the maximal pathological disease state had been reached. This strongly indicates the beneficial role of LtβR–Ig in the delay of demyelination and the acceleration of remyelination. The discrepancy between remyelination rates in these systems could be attributed to developmental abnormalities in the immune systems of *Ltβ*$R^{-/-}$ mice. These findings bode well for the use of an inhibitory LtβR–Ig as a candidate biological therapy in demyelinating disorders, because it is beneficial during both demyelination and remyelination.**

*Key words:* demyelination; cuprizone; glia; Ltαβ; LtβR; therapy

## Introduction

Tumor necrosis factor α (TNFα) and lymphotoxin α (Ltα) (also known as TNFβ) are part of the large TNF superfamily of ligands (Ware et al., 1995; Locksley et al., 2001; Zhang, 2004). Membrane-bound or soluble TNFα signals through TNFRI (also p55) and TNFRII (also p75) to elicit a wide variety of signals in many different cell types. Homotrimeric secreted Ltα also signals through TNFRI and TNFRII. Additionally, Ltα can interact with membrane-bound lymphotoxin β (Ltβ) to form a Ltαβ heterotrimer, which is specific for lymphotoxin β receptor (LtβR) (Crowe et al., 1994; Ware et al., 1995). Signaling through LtβR causes the activation of TNF receptor-associated factor adaptor molecules and induces signals through both the classical and alternative nuclear factor-κB pathways (Baud and Karin, 2001; Dempsey et al., 2003).

The roles of TNFα, Ltα, TNFRI, and TNFRII have been extensively investigated in numerous rodent models of demyelination (Ruddle et al., 1990; Korner et al., 1997; Liu et al., 1998; Probert et al., 2000; Arnett et al., 2001, 2003; Kassiotis and Kollias, 2001). Although TNFα and Ltα are upregulated in multiple sclerosis (MS) and are believed to play an important detrimental role in the pathology of disease (Raine et al., 1998), inhibition of TNFα in patients leads to symptom exacerbation (van Oosten et al., 1996; The Lenercept Multiple Sclerosis Study Group and The University of British Columbia MS/MRI Analysis Group, 1999; Robinson et al., 2001; Sicotte and Voskuhl, 2001), highlighting the need for a comprehensive understanding of the role of TNF family ligands and receptors in demyelinating disease.

Using inhibitors of LtβR signaling to examine the role of LtβR in experimental autoimmune encephalomyelitis (EAE), one report demonstrates that signaling by Ltαβ heterotrimers is important in demyelination (Gommerman et al., 2003). In these studies, T-cell function was believed to be the primary target of LtβR–Ig. Although these results highlight the involvement of in-

Received July 24, 2006; revised June 1, 2007; accepted June 4, 2007.

This work was supported by National Institutes of Health Grants NS34190 (J.P.-Y.T.), NS39508 (M.J.C.), NS045735 (M.J.C.), and DK58891 (Y.-X.F.) and National Multiple Sclerosis Society Grant RG1785 (J.P.-Y.T.). H.A.I. is a fellow of the National Multiple Sclerosis Society (Grant FG1605A). B.P.O. is a fellow of the Irvington Institute for Immunological Research. We thank Jeff Browning and Biogen Idec (Cambridge, MA) for generously supplying LtβR– human IgG-1 Fc, LtβR–mouse IgG-1 Fc, and matched controls human Ig and MOPC-21, as well as providing a critical review of this manuscript.

*S.R.P. and H.A.I. contributed equally to this work.

Correspondence should be addressed to Dr. Jenny P.-Y. Ting, Lineberger Comprehensive Cancer Center, Campus Box 7295, University of North Carolina, Chapel Hill, NC 27599. E-mail: panyun@med.unc.edu.

S. R. Plant's present address: Division of Neurology, Duke University Medical Center, Duke University, Durham, NC 27710.

H. A. Arnett's present address: Department of Inflammation, Amgen, Seattle, WA 98119.

DOI:10.1523/JNEUROSCI.1307-07.2007

 0270-6474/07/277429-09$15.00/0

filtrating T cells in demyelination, the role of CNS-derived Lt$\alpha\beta$ and Lt$\beta$R is not known. In addition, the capacity of signaling via Lt$\beta$R to affect reparative remyelination has not been determined.

In the current investigation, we used the cuprizone model to study the involvement of Lt$\beta$R in demyelination and remyelination. Cuprizone-induced demyelination and remyelination occur without T-cell involvement. We previously used the cuprizone model to demonstrate the detrimental nature of TNF$\alpha$ and Lt$\alpha$ during demyelination and the beneficial effect of TNF$\alpha$ in the remyelination phase (Arnett et al., 2001; Plant et al., 2005). In the present study, we demonstrate detrimental effects of Lt$\beta$R in cuprizone-induced demyelination. In addition, we tested the efficacy of inhibitors of Lt$\beta$R signaling (Lt$\beta$R–Ig) and found significant benefits of blocking the Lt$\beta$R pathway in both demyelination and remyelination phases of the model. These findings strongly suggest that inhibition of Lt$\beta$R signaling in MS patients may be a beneficial treatment option.

## Materials and Methods

*Animals.* C57BL/6 mice were purchased from The Jackson Laboratory (Bar Harbor, ME) and bred in house at the University of North Carolina (UNC) animal facility. *Lt$\beta$R$^{-/-}$* mice (Futterer et al., 1998), previously backcrossed to C57BL/6 for at least five generations, were imported from the University of Chicago and bred in house at the UNC animal facility. All procedures were conducted in accordance with National Institutes of Health guidelines and were approved by the Institutional Animal Care and Use Committee of UNC at Chapel Hill. All mice were 8–10 weeks of age before the start of cuprizone treatment.

*Treatment of mice.* Male *Lt$\beta$R$^{-/-}$* and C57BL/6 wild-type mice were fed *ad libitum* 0.2% cuprizone [oxalic bis(cyclohexylidenehydrazide)] (Sigma-Aldrich, St. Louis, MO) mixed into milled chow. Mice were treated for 3, 3.5, 4, or 5 weeks to study the demyelination process. For remyelination, mice were treated for 6 full weeks with cuprizone and then were returned to a diet of normal pellet chow for 1, 2, 4, or 6 weeks (7, 8, 10, or 12 weeks of total treatment). Untreated mice were maintained on a diet of normal pellet chow. This protocol was used for all studies with the exception of those involving inhibitors of Lt$\beta$R signaling.

Two versions of murine Lt$\beta$R–IgG (Lt$\beta$R–human IgG and Lt$\beta$R–mouse IgG) and their controls were kindly provided by Dr. J. Browning (Biogen Idec, Cambridge, MA) and have been described previously (Gommerman et al., 2003). Separate treatment paradigms were used for studies using Lt$\beta$R–Ig fusion molecules. To study demyelination, mice were intraperitoneally injected on day −1 and weekly thereafter with 5 mg/kg of either Lt$\beta$R–human IgG-1 Fc (Lt$\beta$R–hIg) or human IgG as a control. To study remyelination, a posttreatment paradigm was used, in which mice were treated with cuprizone for 6 full weeks. After 5 weeks plus 2 d of cuprizone treatment (approximate height of demyelination) and weekly thereafter out to 10 weeks, mice were given intraperitoneal injections of either Lt$\beta$R–mouseIgG-1 (Lt$\beta$R–mIg) or matched control mouse IgG-1, MOPC-21. This murine version of Lt$\beta$R–Ig has been shown to be less antigenic in the mouse (J. Browning, personal communication).

*Tissue preparation and histopathological analysis.* Paraffin-embedded coronal brain sections were prepared from the fornix region of the corpus callosum. Luxol fast blue–periodic acid Schiff (LFB–PAS) stained sections were read by three double-blinded readers and graded on a scale from 0 (complete myelination) to 3 (complete demyelination), as described previously (Arnett et al., 2001; Plant et al., 2005).

*Immunohistochemistry.* Detection of mature oligodendrocytes and microglia/macrophages was performed by immunohistochemistry (IHC) as described previously (Plant et al., 2005). Quantitative analyses of glutathione *S*-transferase $\pi$-positive (GST$\pi^+$) and *Ricinus communis* agglutinin-1-positive (RCA-1$^+$) cells were restricted to a 0.033 mm$^2$ area at midline corpus callosum. Only immunopositive cells with an observable 4′,6′-diamidino-2-phenylindole-stained nucleus were included in the quantification. Cell counts are averages of at least 9 and up to 14 mice per time point. Myelinated fibers were detected by immunohistochemistry with a primary antibody to myelin basic protein (MBP) (diluted 1:1000; Sternberger Monoclonals, Lutherville, MD) followed by fluorescein-conjugated anti-mouse IgG (Invitrogen, Carlsbad, CA) diluted 1:1000.

*Dual* in situ *hybridization/immunohistochemical analysis.* After cuprizone treatment, mice were perfused with RNase-free PBS and then 4% paraformaldehyde. Brains were removed and incubated in fixative until mounted for cryosectioning. Detection of mRNA for Lt$\beta$R was performed by *in situ* hybridization (ISH) on free-floating brain cryosections as described previously (Schmid et al., 2002). Briefly, 25 $\mu$m sections were hybridized overnight at 55°C with $^{33}$P-labeled riboprobes ($10^7$ cpm/ml). Excess probe was removed by successive washing with 0.03 M NaCl, 0.003 M sodium citrate (2× SSC) containing 10 mM $\beta$-mercaptoethanol ($\beta$-ME), followed by a 1 h incubation with ribonuclease at 37°C, a 2 h incubation at 55°C with 0.5× SSC, 50% formamide, and 10 mM $\beta$-ME, and finally by a 1 h incubation at 68 C in 0.1× SSC, 5 mM $\beta$-ME and 5% sarcosyl. Myeloid cells and blood vessels were identified by their ability to bind biotinylated tomato lectin (Sigma, St. Louis, MO), and visualized by standard streptavidin–horseradish peroxidase methodology. Tissue sections were air dried onto superfrost plus slides (Fisher Scientific, Hampton, NH) and coated with Ilford K-5 emulsion (Polysciences, Warrington, PA). After 3 weeks, the emulsion-coated slides were developed with Kodak D19 developer and fixative (Fisher Scientific). Mayer's hematoxylin was used to visualize cellular nuclei, before dehydrating and preserving tissues sections under glass coverslips with Permount. Emulsion grains were counted in six microscopy fields per tissue section. Tissue sections from at least three mice were quantified. In each experiment, the basal (nonspecific) levels of grain counts were determined from quantifying grains over ventricles and areas without tissues. Induced expression was defined as threefold increase in grains per microscopic field.

To discern the cell types that express Lt$\beta$R, the same tissue sections were also immunolabeled with either tomato lectin to visualize microglia, macrophages, and blood vessels or antibody to glial fibrillary acidic protein (GFAP) to visualize astrocytes. All immunolabeled cells were visualized by horseradish peroxidase staining (indicated by brown stain), whereas cells expressing the Lt$\beta$R transcript were identified by black grains generated by *in situ* hybridization. Blood vessels are readily distinguished from microglia and macrophages by their tubular structure. Tomato lectin does not distinguish between microglia and macrophages.

*Reverse transcription-PCR and quantitative real-time reverse transcription-PCR.* Total RNA was isolated from a dissected region of the brain containing the corpus callosum of wild-type and *Lt$\beta$R$^{-/-}$* mice at several points during and after cuprizone treatment. RNA isolation was performed using the Qiagen (Valencia, CA) RNeasy kit under RNase-free conditions. Reverse transcription (RT)-PCR for LIGHT (homologous to lymphotoxins, exhibits inducible expression, and competes with herpes simplex virus glycoprotein D for the herpes-virus entry mediator, a receptor expressed by T lymphocytes) was performed in 20 $\mu$l reactions using the following primers: 5′ primer, CTGGCATGGAGAGTGTGGTA; 3′ primer, GATACGTCAAGCCCCTCAAG.

TaqMan 5′ nuclease quantitative real-time PCR assays were performed using an ABI Prism 7900 sequence-detection system (Applied Biosystems, Foster City, CA) in a 15 $\mu$l reaction with universal master mix (Invitrogen), 200 nM Lt$\beta$R target primers, and 100 nM probe. Lt$\beta$R-specific primers were designed to span intron–exon junctions to differentiate between cDNA and genomic DNA. The primers and probe used to detect mouse Lt$\beta$R were as follows: 5′ primer, GTACTCTGCCAGCCTGGCACAGAAGCCGAGGTCACAGATG; 3′ primer, GGTATGGGGTTGACAGCGGGCTCGAGGGGAGG; probe, 6-carboxyfluorescein (Fam)-ACGTCAACTGTGTCCC-6-carboxytetramethylrhodamine (Tamra). The primers and probe for mouse 18S ribosomal RNA were as follows: 5′ primer, GCTGCTGGCACCAGACTT; 3′ primer, CGGCTACCACATCCAAGG; probe, Fam-CAAATTACCCACTCCCGACCCG-Tamra. Thermal cycle parameters were optimized to 2 min at 50°C, 2 min at 95°C, and 40 cycles comprising denaturation at 95°C for 15 s and annealing–extension at 56°C for 1.5 min. Reactions for 18S were performed alongside Lt$\beta$R during each experiment and used to normalize for amounts of cDNA.

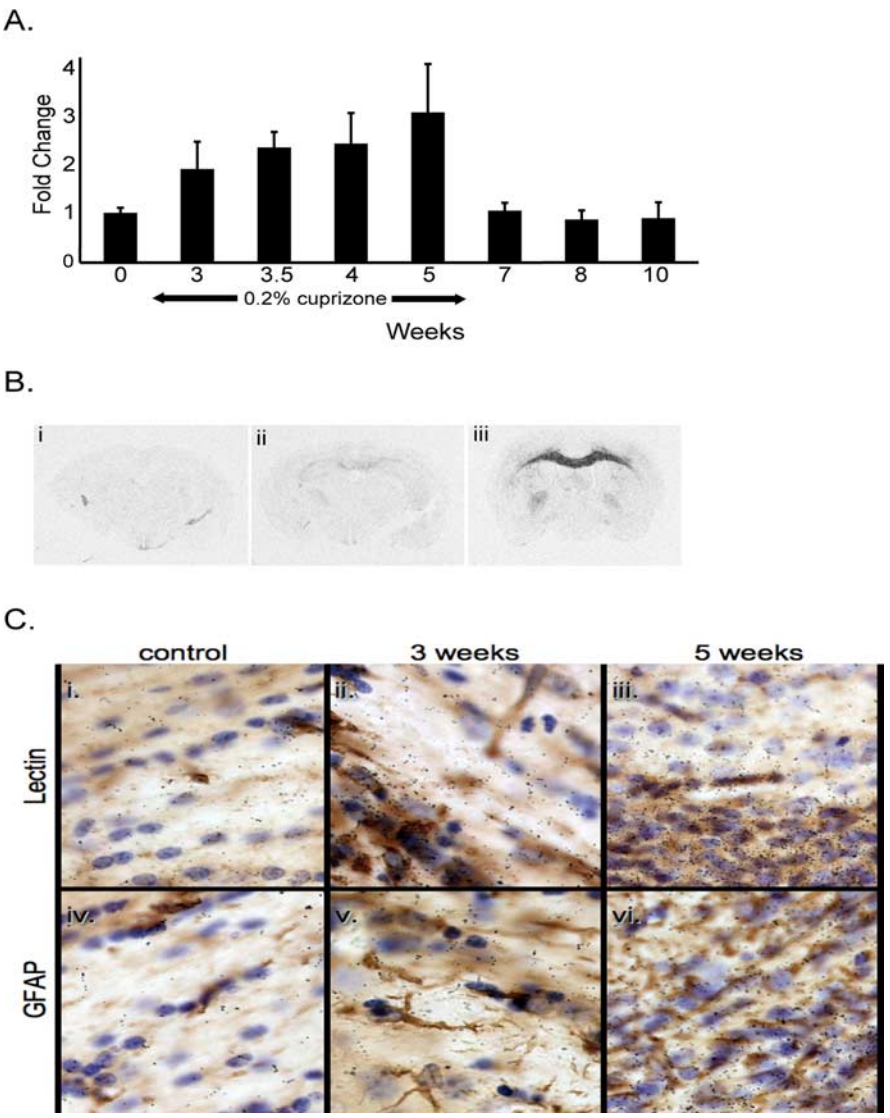


**Figure 1.** Upregulation of Lt$\beta$R during demyelination and inflammation. ***A***, Upregulation of Lt$\beta$R during demyelination and inflammation. Quantitative real-time RT-PCR analysis demonstrates an upregulation of Lt$\beta$R mRNA expression in wild-type mice during cuprizone treatment (through week 5) and a decline to baseline levels during remyelination (weeks 7–10). ***B***, Localization of Lt$\beta$R mRNA by ISH during cuprizone treatment. At the level of autoradiogram analysis, Lt$\beta$R mRNA expression is not detected by *in situ* hybridization in brains from untreated wild-type mice (***i***). Induction of Lt$\beta$R mRNA is weakly detected within the corpus callosum of mice treated for 3 weeks (***ii***), and robust induction of Lt$\beta$R is seen in the same regions in brains from mice treated for 5 weeks (***iii***). ***C***, Microscopic examination of the same brain sections shows Lt$\beta$R expression is highest in regions and time points with a large accumulation of microglia/macrophages. In ***i–vi***, nuclei are visualized by hematoxylin (blue) and Lt$\beta$R expression by $^{33}$P-labeled riboprobes (dark grains within the emulsion). In ***i–iii***, microglia, blood vessels, and macrophages are visualized with tomato lectin (brown), whereas in ***iv–vi***, astrocytes are visualized with GFAP antibodies (brown). In all panels, the focal plane is optimized to visualize the riboprobe-induced grains within the emulsion.

*Statistical analysis.* Unpaired Student's *t* tests were used to statistically evaluate significant differences. Data are expressed as mean ± SEM.

## Results

### Lt$\beta$R and LIGHT expression in the brain

To assess Lt$\beta$R expression in the cuprizone model, we performed quantitative real-time RT-PCR to examine the level of Lt$\beta$R in the corpus callosum and surrounding tissue in untreated and cuprizone-treated mice. Low levels of Lt$\beta$R were detected in control untreated mice, whereas the levels of Lt$\beta$R rose moderately throughout demyelination but were then reduced to baseline levels during the remyelination phase (Fig. 1*A*).

Numerous strategies to detect Lt$\beta$R protein expression were used, including immunoblot, IHC, and flow cytometry. Unfortunately, high-quality specific antibodies for the detection of mouse Lt$\beta$R by immunoblot or IHC have not been reported, and we verified that existing antibodies do not work in these assays. Although antibodies for flow cytometry have been reported (Crowe et al., 1994; Dejardin et al., 2002) for the staining of immune cells, flow cytometry of adult brain cells is exceedingly challenging, and the results appear suboptimal. Nonetheless, we performed flow cytometry for microglial ($CD45^+CD11b^+$) and astroglial ($GFAP^+$) cell populations but were unable to obtain specific staining for Lt$\beta$R by comparing brain cells isolated from wild-type versus $Lt\beta R^{-/-}$ mice (supplemental Fig. 1, available at www.jneurosci.org as supplemental material). Because of the lack of appropriate serological reagents for the detection of Lt$\beta$R protein, dual ISH/IHC analysis was used to simultaneously define the regions expressing the Lt$\beta$R transcript and identify cell populations present in these regions during cuprizone treatment. Lt$\beta$R mRNA expression was not detected in the CNS of untreated mice (Fig. 1*Bi*). By 3 weeks of cuprizone treatment, a low level of Lt$\beta$R expression was detected in the corpus callosum region (Fig. 1*Bii*). By 5 weeks of treatment, robust expression of Lt$\beta$R was detected throughout the corpus callosum and slightly weaker expression was detected in the striatal regions (Fig. 1*Biii*). By 3 weeks of cuprizone treatment, there was an increase in the hypercellularity of tomato lectin-stained cells in the corpus callosum, and this level was further enhanced at the 5 week time point, consistent with previous observations of robust microgliosis (Fig. 1*Cii*,*Ciii*). Comparison of regions with prominent microglia/macrophage accumulation at both time points revealed that robust Lt$\beta$R ISH signal (black grains) was enhanced in all regions with strong induction of tomato lectin staining indicated by the brown coloration. Enhanced expression is defined as a threefold increase from controls in grain density. In a different set of samples, astrogliosis indicated by increased brown color attributed to GFAP immunoreactivity was observed at the 3 week time point, and it also became much more evident at the 5 week time point (Fig. 1*Cv*,*Cvi*). At the 3 week time point, there was little colocalization of grains with $GFAP^+$ cells (Fig. 1*Cv*), but, at the 5 week time point (Fig. 1*Cvi*), $GFAP^+$ cells were accompanied by Lt$\beta$R grains. This indicates that, at the 3 week time point before the dramatic increase in hypercellularity, Lt$\beta$R expression is preferentially detected in regions enriched for lectin-positive cells (Fig. 1, compare *Cii*, *Cv*). However, after 5 weeks of treatment, Lt$\beta$R expression is most intense in areas enriched for microglia/macrophages, but it is also increased in areas of astrogliosis.

Because the membrane-bound ligand LIGHT (Granger and Ware, 2001) has the ability to interact with Lt$\beta$R, at least in the periphery, we analyzed LIGHT expression levels by RT-PCR during cuprizone treatment. Although LIGHT is found at high levels in the control spleen and thymus, negligible levels were found in the brains of untreated or cuprizone-treated mice (Fig. 2*A*). In addition, LIGHT is not regulated by the presence of Lt$\beta$R because mice lacking Lt$\beta$R express similar levels of LIGHT in the brain (Fig. 2*B*). This suggests that LIGHT does not play a significant role during cuprizone-induced inflammation. This is similar to the conclusion reached by others using the EAE model (Gommerman et al., 2003).

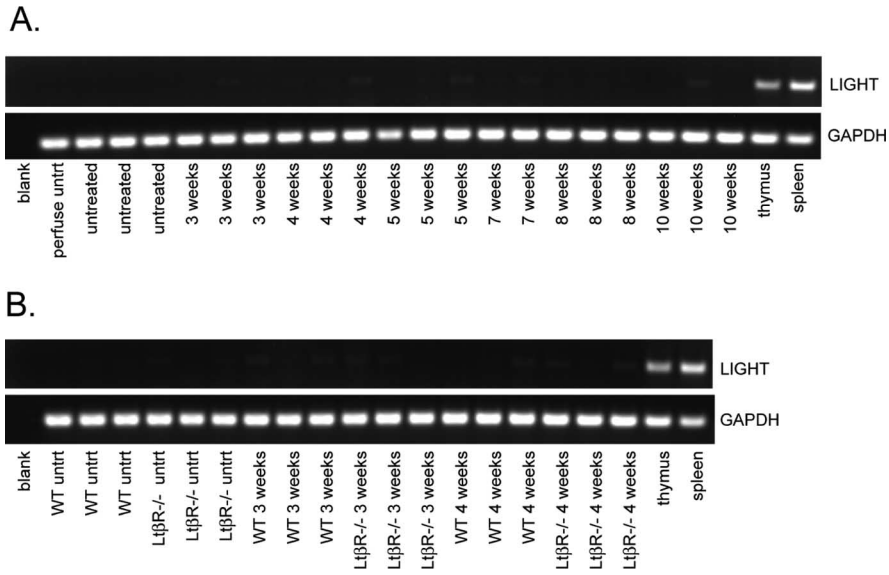


**Figure 2.** PCR analysis of LIGHT during cuprizone treatment. ***A***, RT-PCR for the ligand LIGHT was performed on cDNA from untreated and cuprizone-treated wild-type mouse brain. As controls, untreated thymus and spleen were analyzed. Representative results show that very low levels of LIGHT mRNA exist in the untreated and cuprizone-treated brain. ***B***, RT-PCR on wild-type (WT) and *Lt$\beta$R$^{-/-}$* untreated (untrt) and treated brain cDNA demonstrate that the lack of Lt$\beta$R has no effect on LIGHT RNA levels.

### Delayed demyelination in *Lt$\beta$R$^{-/-}$* mice

To analyze the role of Lt$\beta$R in demyelination, cuprizone-treated *Lt$\beta$R$^{-/-}$* mice were compared with treated wild-type mice. A significant delay in demyelination was observed in the *Lt$\beta$R$^{-/-}$* mice relative to wild-type mice, as assessed by LFB–PAS staining (Fig. 3*A*). These data indicate that signaling through Lt$\beta$R exacerbates the inflammatory demyelinating process. This delay could be seen as early as 3 weeks ( $p < 0.02$) of cuprizone treatment but was most pronounced at 3.5 weeks ( $p < 0.01$) and 4 weeks ( $p < 0.001$) of treatment and is clearly revealed by representative LFB–PAS images of wild-type and *Lt$\beta$R$^{-/-}$* mice at 4 weeks of treatment (Fig. 3*B*). Because the delay in demyelination in *Lt$\beta$R$^{-/-}$* mice is similar to the delay in demyelination seen in *Lt$\alpha^{-/-}$* mice (Plant et al., 2005), this suggests that membrane-bound Lt$\alpha\beta$ signaling through the Lt$\beta$R is involved in the demyelination process.

### Delayed remyelination in *Lt$\beta$R$^{-/-}$* mice

The ability of mature oligodendrocytes to remyelinate the corpus callosum was studied in LFB–PAS-stained paraffin sections from wild-type and *Lt$\beta$R$^{-/-}$* mice. Modest but significant differences in remyelination were observed between wild-type and *Lt$\beta$R$^{-/-}$* mice at 7 weeks ( $p < 0.001$) and 10 weeks ( $p < 0.02$) (Fig. 3*A*). By 12 weeks, *Lt$\beta$R$^{-/-}$* mice have remyelinated to the same extent as wild-type controls ( $p = 0.11$). These differences during remyelination are $<0.5$ on the scale of severity of demyelination, whereas differences seen in studies of *TNF$\alpha^{-/-}$* versus wild-type mice were $>1.5$ on the scale (Arnett et al., 2001) and persisted up to 14 weeks (our unpublished data). We conclude that, although remyelination appears to be transiently delayed in *Lt$\beta$R$^{-/-}$* mice, it eventually occurs.

### Delayed loss of oligodendrocytes in *Lt$\beta$R$^{-/-}$* mice during demyelination

To verify that the delay in demyelination observed by LFB–PAS is accompanied by changes in oligodendrocyte number, we performed immunohistochemistry for GST$\pi$, a marker shown to be specific for mature myelinating oligodendrocytes (Tansey and Cammer, 1991) on adjacent paraffin sections. GST$\pi^+$ cells at the midline corpus callosum were quantitated. Abundant oligodendrocytes were detected in both wild-type and *Lt$\beta$R$^{-/-}$* untreated mice. As has been shown previously, the number of GST$\pi^+$ oligodendrocytes is dramatically reduced after 3 weeks of cuprizone treatment (Mason et al., 2000; Arnett et al., 2002). This represents an actual loss of oligodendrocytes because these cells exhibit increased apoptosis rather than a simple loss of the marker (Arnett et al., 2002). However, after 3.5 weeks of treatment, significantly more oligodendrocytes were present in *Lt$\beta$R$^{-/-}$* mice compared with wild-type mice ( $p < 0.01$) (Fig. 4*A*,*B*), indicating a delay in the death of oligodendrocytes in the absence of Lt$\beta$R. No difference in oligodendrocyte number was found between wild-type and *Lt$\beta$R$^{-/-}$* mice at 4 weeks. These data are complementary to the LFB staining results (Fig. 3*A*). By 5 weeks of cuprizone treatment, few GST$\pi^+$ oligodendrocytes were detected in the corpus callosum of wild-type and *Lt$\beta$R$^{-/-}$* mice. This data point is consistent with the severe demyelination shown in Figure 3*A* for both mouse strains at the 5 week time point.

### Normal oligodendrocyte repopulation of corpus callosum in *Lt$\beta$R$^{-/-}$* mice during remyelination

Although oligodendrocytes were rarely detected in the corpus callosum of 5 week cuprizone-treated mice, just 1 week after the removal of cuprizone (7 weeks), the corpus callosum was repopulated to ~75% of the original number of mature oligodendrocytes. No difference in oligodendrocyte number was observed between wild-type and *Lt$\beta$R$^{-/-}$* mice. By week 10, the number of mature oligodendrocytes residing in the corpus callosum recovered to pretreatment levels in both wild-type and *Lt$\beta$R$^{-/-}$* mice. Thus, Lt$\beta$R is not required for oligodendrocyte progenitor proliferation and maturation during the remyelination phase. This differs from our previous study that demonstrated a profound role for TNF$\alpha$ and TNFRII in the proliferation of oligodendrocyte progenitors (Arnett et al., 2001).

### Recruitment of microglia/macrophage is not changed in *Lt$\beta$R$^{-/-}$* mice

Cuprizone induces a chronic inflammatory state in the brain including the recruitment of activated microglia and macrophages to the sites of insult (Matsushima and Morell, 2001). Par-

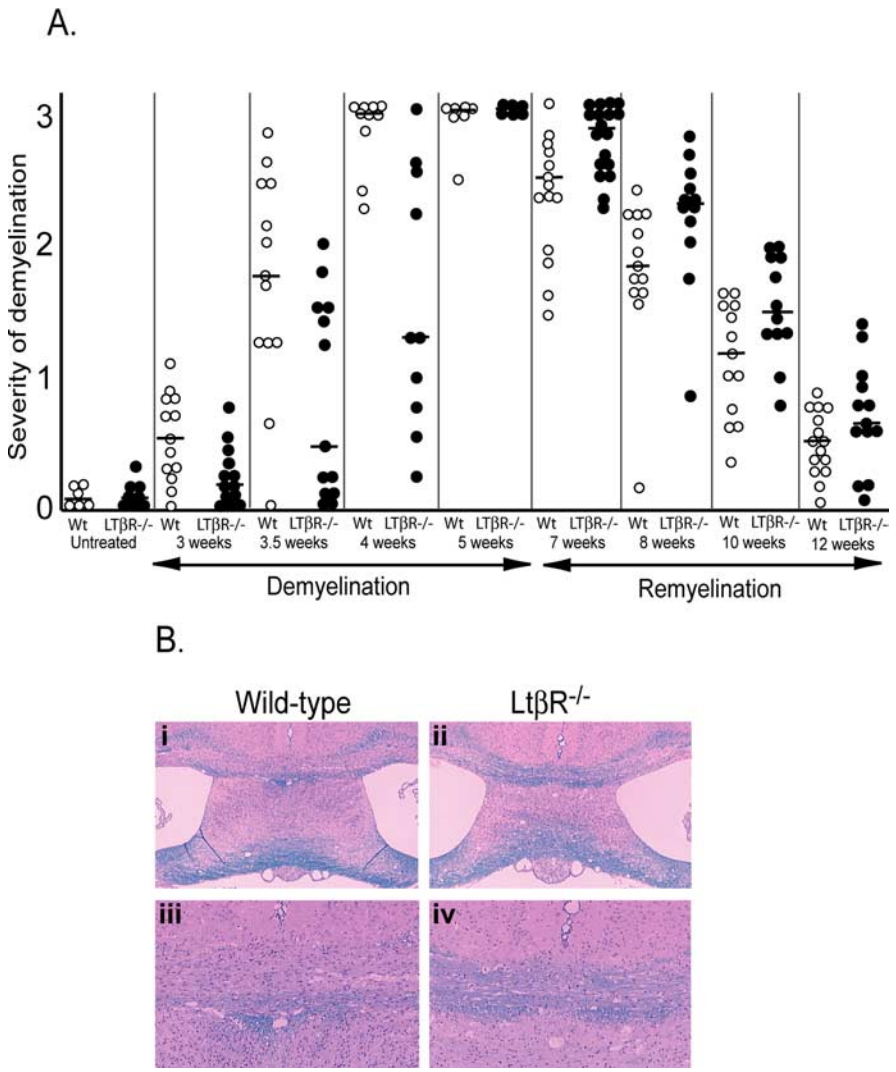


**Figure 3.** Time course of demyelination and remyelination in $Lt\beta R^{-/-}$ and wild-type mice. ***A***, LFB–PAS-stained paraffin sections were graded on a scale from 0 (normal myelination) to 3 (complete demyelination) by three double-blinded investigators. Each circle represents an individual mouse: open circles, C57BL/6 wild-type (Wt); filled circles, $Lt\beta R^{-/-}$ mice. Horizontal lines indicate the median score of each group. Significant differences in demyelination were seen between wild-type and $Lt\beta R^{-/-}$ mice at 3 weeks ( $p < 0.02$), 3.5 weeks ( $p < 0.01$), and 4 weeks ( $p < 0.001$). Significant differences during remyelination were detected at 7 weeks ( $p < 0.001$) and 10 weeks ( $p < 0.02$). ***B***, Representative LFB–PAS pictures at 4 weeks of treatment demonstrate the delay in demyelination in $Lt\beta R^{-/-}$ mice (***ii***) compared with wild-type mice (***i***). Higher-magnification images of the corpus callosum of $Lt\beta R^{-/-}$ (***iv***) and wild-type (***iii***) mice demonstrate the lack of myelinated fibers and increased inflammation in wild-type mice during demyelination.

affin sections from $Lt\beta R^{-/-}$ and wild-type mice were stained with the lectin RCA-1, and microglia/macrophages at midline corpus callosum were quantitated. We found no difference between $Lt\beta R^{-/-}$ and wild-type mice in the recruitment of activated microglia/macrophage during the demyelination or remyelination phases of this model (Fig. 4*C*).

### Inhibition of functional Lt$\beta$R reduces demyelination

It has been well established that mice lacking Lt$\beta$R from birth have significant developmental abnormalities (Futterer et al., 1998). Functional inhibition of Lt$\beta$R in wild-type mice is possible using a fusion decoy protein and has been shown to affect the time course of EAE as well as prevent disease relapse (Gommerman et al., 2003). To assess the validity of our findings in $Lt\beta R^{-/-}$ mice demonstrating a detrimental role for Lt$\beta$R during cuprizone-induced demyelination, we treated C57BL/6 mice with either Lt$\beta$R–hIg fusion decoy protein or control human IgG during cuprizone treatment. Lt$\beta$R–hIg was shown previously to effectively inhibit Lt$\alpha\beta$–Lt$\beta$R signaling (Gommerman et al., 2003). Mice were pretreated with either Lt$\beta$R–hIg or control human Ig 1 d before start of the cuprizone (day −1) and weekly thereafter by intraperitoneal injection (5 mg/kg) and were maintained on an *ad libitum* diet of 0.2% cuprizone for 3.5 weeks (Fig. 5*A*). Mice were then perfused, and paraffin brain sections were stained with LFB–PAS to assess the extent of demyelination at the midline corpus callosum. Mice treated with control human Ig were significantly more demyelinated than mice that received the Lt$\beta$R–hIg inhibitor ( $p < 0.02$) (Fig. 5*B*,*Ci*–*Civ*). Immunohistochemistry for MBP confirmed the increase of myelinated fibers in mice treated with Lt$\beta$R–hIg relative to mice treated with control human Ig. In conclusion, demyelination in cuprizone-treated mice can be significantly delayed by inhibition of Lt$\beta$R. This is similar to the effect observed in the EAE disease models using both mice and rats (Gommerman et al., 2003). Our data demonstrates that Lt$\beta$R–hIg can reduce demyelination in a model without T-cell involvement.

### Inhibition of Lt$\beta$R enhances remyelination

Because our goal is to enhance the development of a therapeutic treatment for demyelinating disease, we investigated the ability of Lt$\beta$R–Ig to alter the extent of remyelination after significant demyelination had already occurred. To investigate the role of Lt$\beta$R in the process of remyelination, C57BL/6 mice were treated with cuprizone for 6 weeks. This period of cuprizone treatment reproducibly results in complete demyelination in all mice studied to date, including the wild-type C57BL/6 mice (Arnett et al., 2001; Plant et al., 2005). Because of the concern that human Fc might elicit an immune response in this prolonged experiment, a fusion protein consisting of Lt$\beta$R–mIg was used in these studies. After 5 weeks plus 2 d of cuprizone treatment and weekly thereafter, mice were injected intraperitoneally with either Lt$\beta$R–mIg or control mouse IgG-1. Cuprizone treatment was halted at the 6 week time point, and mice were returned to normal chow (Fig. 6*A*). Mice were killed after 10 weeks, and LFB-stained sections were analyzed as described above. Remarkably, mice treated with Lt$\beta$R–mIg showed significantly enhanced remyelination ( $p < 0.007$) relative to mice treated with the control mouse Ig as measured by LFB staining (Fig. 6*B*,*Ci*–*Civ*). Additionally, immunohistochemistry for MBP confirmed increased remyelination in mice treated with Lt$\beta$R–mIg compared with control mouse Ig-treated mice (Fig. 6*Cv*,*Cvi*). The number of mature oligodendrocytes within the corpus callosum at 10 weeks was also quantitated. GST$\pi$-

positive oligodendrocytes were modestly more prevalent in the corpus callosum of Lt$\beta$R–mIg-treated mice compared with control mouse Ig-treated mice, and this difference is statistically significant ( $p < 0.04$) (Fig. 6*Cvii*,*Cviii*). In conclusion, remyelination in cuprizone-treated mice was significantly enhanced by posttreatment with an inhibitor of Lt$\beta$R signaling.

## Discussion

The results of our study demonstrate an exacerbatory role for Lt$\beta$R in cuprizone-induced oligodendrocyte death and demyelination. Furthermore, they show a beneficial role of inhibitory Lt$\beta$R–Ig proteins in both the demyelination and remyelination phases of this model. Initially, our comparison of *Lt$\beta$R$^{-/-}$* and wild-type mice demonstrates a strong exacerbatory role for Lt$\beta$R during the demyelination phase, suggesting Lt$\beta$R as a possible therapeutic target for treating demyelinating disorders. However, the moderate delay observed in *Lt$\beta$R$^{-/-}$* mice during remyelination raised concerns regarding the potential efficacy of using Lt$\beta$R inhibitors to treat such disorders. Because of the severe developmental abnormalities in *Lt$\beta$R$^{-/-}$* mice, it was necessary to directly analyze Lt$\beta$R inhibition in mice with an otherwise functional immune system and without the developmental abnormalities seen in *Lt$\beta$R$^{-/-}$* mice. The most important result of this study is the significant delay in demyelination and acceleration of remyelination induced by Lt$\beta$R–Ig treatment of wild-type mice. The latter was observed in a posttreatment paradigm (Fig. 6). Despite the fact that mice exhibited complete demyelination at the initiation of posttreatment, Lt$\beta$R–mIg significantly enhanced remyelination relative to treatment with control mouse Ig.

We recently reported that the presence of Lt$\alpha$ exacerbated demyelination induced by cuprizone treatment (Plant et al., 2005). We further showed that the lack of Lt$\alpha$ did not alter the course of remyelination or the proliferation of oligodendrocyte progenitors during the remyelination phase of the cuprizone model. Lt$\alpha$ can function as a homotrimeric molecule signaling through the TNF receptors, as well as a heterotrimeric molecule with Lt$\beta$ to signal through the Lt$\beta$R. The role of TNF receptors in the cuprizone model has been analyzed previously (Arnett et al., 2001), but the role of Lt$\beta$R in this model was unknown before this study.

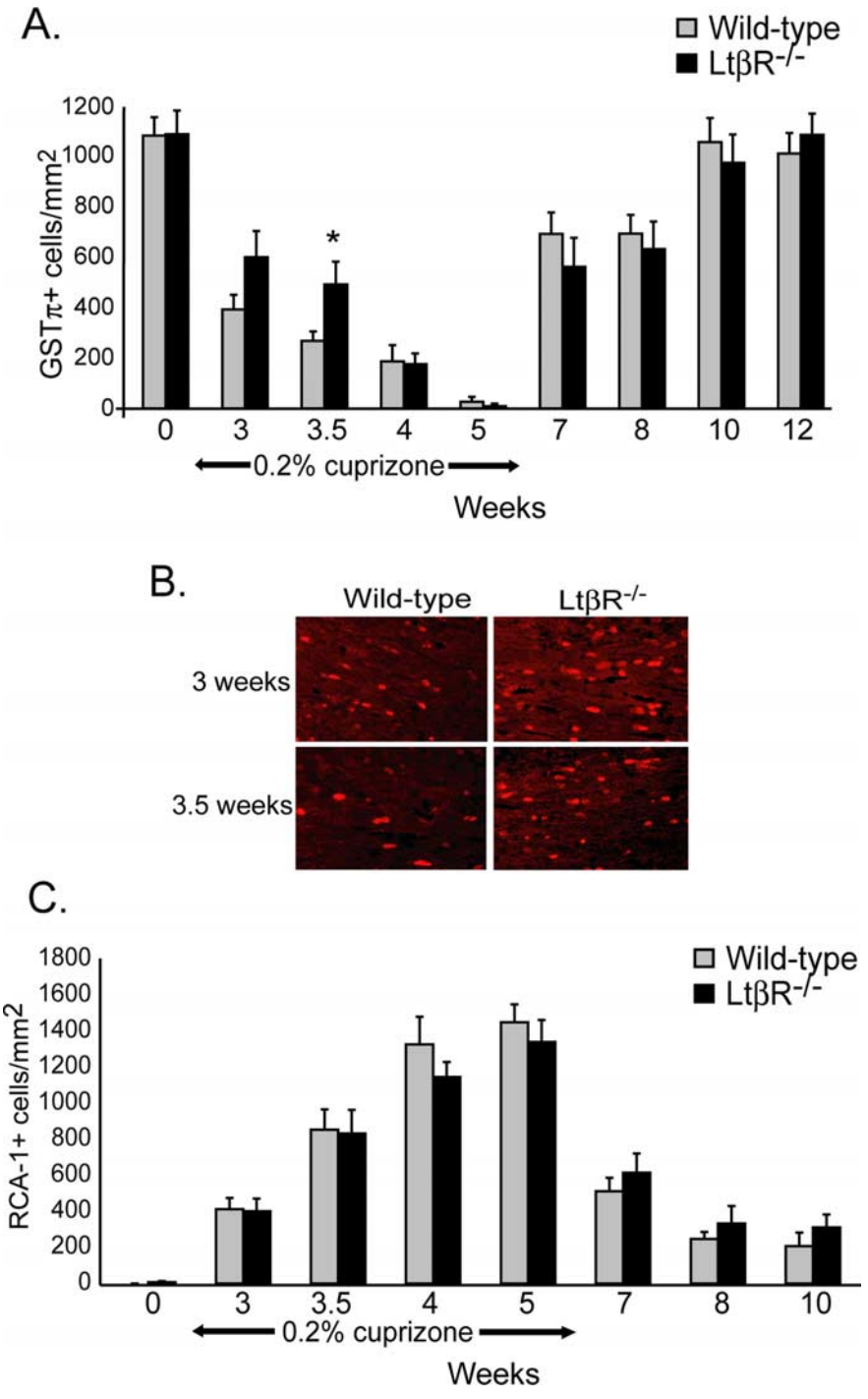


**Figure 4.** Delayed loss of mature oligodendrocytes during demyelination in *Lt$\beta$R$^{-/-}$* mice. ***A***, Mature oligodendrocytes were detected at midline corpus callosum of wild-type and *Lt$\beta$R$^{-/-}$* brains by GST$\pi$ immunohistochemistry. More GST$\pi^+$ cells were found in *Lt$\beta$R$^{-/-}$* mice compared with wild-type mice at 3 weeks ( $p = 0.09$) (wild-type, gray bars; *Lt$\beta$R$^{-/-}$*, black bars). Significantly more GST$\pi^+$ cells were found in *Lt$\beta$R$^{-/-}$* mice at 3.5 weeks ( $p < 0.03$), although no differences in oligodendrocytes were found at 4 and 5 weeks of cuprizone treatment. After the removal of cuprizone, no differences in oligodendrocyte repopulation of the corpus callosum were observed between wild-type and *Lt$\beta$R$^{-/-}$* mice. ***B***, Representative pictures of GST$\pi^+$ cells from wild-type and *Lt$\beta$R$^{-/-}$* mice at 3 and 3.5 weeks of cuprizone treatment. ***C***, Microglial/macrophage accumulation at midline corpus callosum is unaffected by Lt$\beta$R. Microglia/macrophages were detected by RCA-1 lectin staining of paraffin sections from wild-type and *Lt$\beta$R$^{-/-}$* mice during demyelination and remyelination time points. No significant difference in numbers of RCA-1$^+$ cells was observed between wild-type and *Lt$\beta$R$^{-/-}$* mice at any time point.

Studies to assess the role of Lt$\beta$R in normal or pathological states involving the CNS are limited. Using the Theilers murine encephalomyelitis virus model of demyelination, it has been shown that Lt$\alpha$ and Lt$\beta$R are important for viral clearance and the prevention of demyelination within the CNS, but this role is primarily mediated by functional cytotoxic T cells, which require Lt$\alpha$ and Lt$\beta$R for their development (Lin et al., 2003). Specific

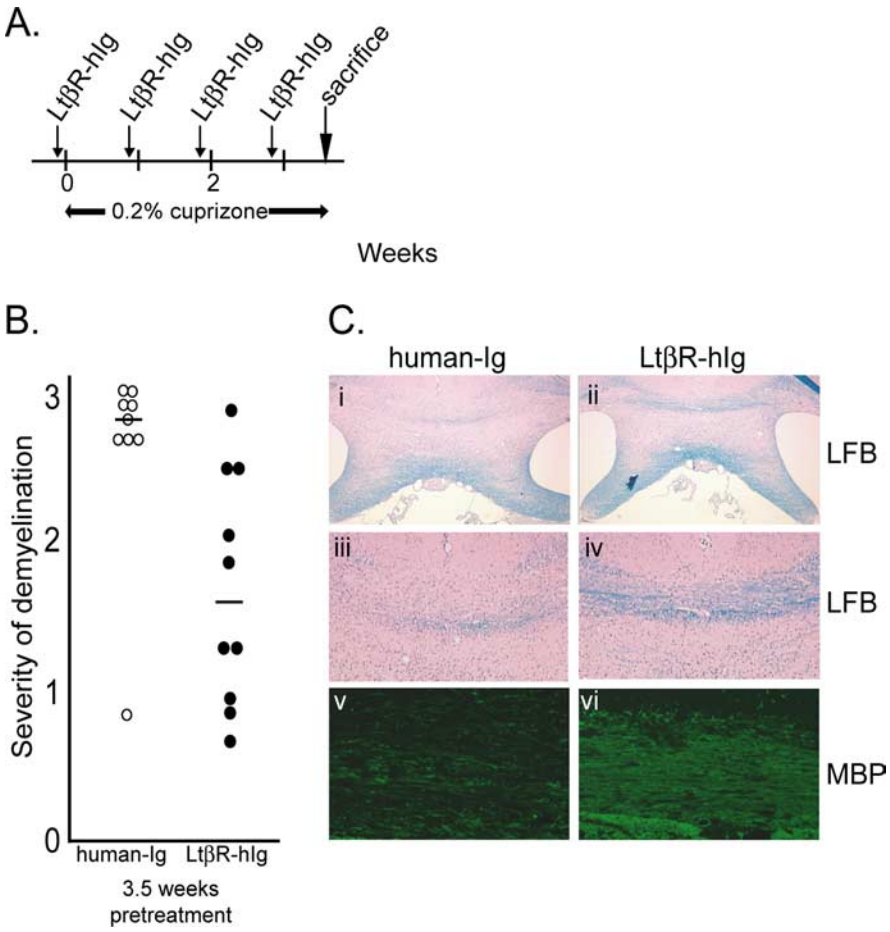


**Figure 5.** Therapeutic inhibition of Lt$\beta$R significantly delays demyelination. ***A***, C57BL/6 mice were treated with 0.2% cuprizone for 3.5 weeks. Mice received weekly injections (indicated by small arrows) of either Lt$\beta$R– hIg or control human Ig beginning at day −1 of cuprizone treatment. ***B***, Significant differences in demyelination were observed between Lt$\beta$R– hIg-treated and control human Ig-treated mice after 3.5 weeks of cuprizone treatment ( $p < 0.02$). LFB–PAS-stained paraffin sections were graded on a scale of 0 (normal myelination) to 3 (complete demyelination) by three double-blinded investigators. Each circle represents an individual mouse: open circles, control human Ig-treated mice; filled circles, Lt$\beta$R– hIg-treated mice. Horizontal lines indicate the median score of each group. ***C***, Representative LFB–PAS pictures at 3.5 weeks of treatment demonstrate the delay in demyelination in control human Ig-treated mice (***i***) compared with Lt$\beta$R– hIg-treated mice (***ii***). High-magnification images of the corpus callosum of control human Ig-treated mice (***iii***) and Lt$\beta$R– hIg-treated mice (***iv***) demonstrate the lack of myelinated fibers and increased inflammation in control human Ig-treated mice during demyelination. Immunohistochemistry for MBP confirmed the presence of more myelinated fibers in Lt$\beta$R– hIg-treated mice (***vi***) compared with control human Ig-treated mice (***v***).

Lt$\beta$R pathway inhibitors administered in the EAE model revealed a detrimental role of Lt$\alpha\beta$–Lt$\beta$R signaling in demyelination, although the major cellular players in this model are also T cells (Gommerman et al., 2003).

In contrast to the above-mentioned disease models, cuprizone-induced demyelination is not a T-cell-mediated event. T cells are not prevalent during cuprizone-induced demyelination, and the onset of demyelination and remyelination is similar in recombination activating gene *RAG-1*$^{-/-}$ mice that lack T and B cells (Arnett et al., 2001; Matsushima and Morell, 2001). Although the CD4$^+$ T-cell-mediated EAE models have provided significant insight, they have not always had predictive value for MS therapies. Furthermore, there is evidence to suggest that MS is not strictly a CD4$^+$ Th1-mediated disease (Lassmann and Ransohoff, 2004), and some demyelinating lesions can be found in the brain that do not coincide with T-cell infiltration but are marked by glial infiltrates (Lucchinetti et al., 2000; Peterson et al., 2001; Barnett and Prineas, 2004). The demyelinating lesions in the cuprizone model of demyelination are also characterized by massive microglia/macrophage and astrocyte infiltrates without evidence of T cells and thus effectively mimic this subtype of MS lesion. Strikingly, in this report we also find Lt$\beta$R upregulation primarily in the corpus callosum in which massive inflammation and demyelination is consistently observed (Fig. 1*B*). By *in situ* hybridization, Lt$\beta$R was localized to areas enriched for activated microglia/macrophages (Fig. 1*C*), although some expression is also found in astroglial-enriched regions, suggesting that Lt$\beta$R on glial cells actively participates in inflammation and demyelination during cuprizone treatment. The fact that mice lacking functional Lt$\beta$R show delayed onset of demyelination reinforces this possibility.

In a previous publication, we used an antibody against Lt$\alpha$ to unequivocally demonstrate Lt$\alpha$ expression by astrocytes in the inflamed corpus callosum of cuprizone-treated mice (Plant et al., 2005). This result coupled with the present finding that microglia are a major source of Lt$\beta$R expression suggests that Lt$\alpha\beta$–Lt$\beta$R signaling between astrocytes and microglia is a primary mediator in the inflammatory demyelinating process that occurs during cuprizone treatment. In addition to Lt$\alpha\beta$, Lt$\beta$R interacts with the membrane-bound ligand LIGHT. LIGHT has been studied to a lesser extent but appears to be localized primarily to T cells, immature dendritic cells, granulocytes, and monocytes (Gommerman and Browning, 2003). We show that LIGHT is present at very low to undetectable levels in the brain, and its expression level is not altered by the presence of Lt$\beta$R or by cuprizone treatment (Fig. 2). These data suggest a scenario in which the Lt$\alpha$ produced by activated astrocytes binds and activates Lt$\beta$R on microglia/macrophages. Because Lt$\alpha$ is known to signal through Lt$\beta$R in a heterotrimeric membrane-bound complex with Lt$\beta$ and not in the soluble Lt$\alpha$ form (Ware et al., 1995), this interaction likely requires cell-to-cell contact at the site of inflammation and demyelination. The present study indicates that glial-derived Lt$\alpha\beta$–Lt$\beta$R signaling plays an important role in the demyelination process. Considering the large numbers of microglia and astrocytes that infiltrate the corpus callosum from 3–6 weeks of cuprizone treatment, this cell–cell interaction is highly plausible (Hiremath et al., 1998; Matsushima and Morell, 2001).

Our data obtained in *Lt$\beta$R*$^{-/-}$ mice indicate that Lt$\beta$R has a significant exacerbatory effect on demyelination and a potentially modest beneficial effect during remyelination. This result is similar to our previous findings using *Lt$\alpha$*$^{-/-}$ mice with respect to demyelination, but *Lt$\alpha$*$^{-/-}$ mice remyelinated normally (Plant et al., 2005). There is evidence that mice lacking Lt$\beta$R from birth have significant developmental abnormalities; *Lt$\beta$R*$^{-/-}$ mice lack mesenteric lymph nodes, Peyer's patches, and colon-

associated lymphoid tissues. In addition, T- and B-cell segregation is lost, follicular dendritic cell networks are not defined in the spleen, and antibody affinity maturation is defective (Futterer et al., 1998). It is known that Lt$\beta$R exerts control over chemokine and cytokine synthesis (Chin et al., 2003), although the full impact on the CNS is not known. Furthermore, natural killer cells in $Lt\beta R^{-/-}$ mice do not have surface expression of the NK1.1 receptor attributable to the proximity of the encoding gene and the *Ltbr* gene (Wu et al., 2001). For these reasons, it is possible that our results with $Lt\beta R^{-/-}$ mice do not accurately reflect the true role of Lt$\beta$R in inflammation and demyelination attributable to the developmental abnormalities found in $Lt\beta R^{-/-}$ mice.

Lt$\beta$R–Ig inhibitors have been successful in reducing disease severity in the EAE model of demyelination (Gommerman et al., 2003). The same inhibitory fusion Igs were used in conjunction with the cuprizone model here to analyze the effect of functional Lt$\beta$R inhibition in wild-type C57BL/6 mice. Compared with human Ig protein-treated mice, Lt$\beta$R–hIg-treated mice exhibited a significant delay in demyelination after 3.5 weeks of cuprizone treatment (Fig. 5*B*,*C*), providing support for the Gommerman et al. study (2003). Variations observed between wild-type mice in these studies are within the normal range for the cuprizone model (Figs. 3, 5, 6), and, for this reason, wild-type animals are included in each experiment. However, this study was undertaken using an EAE model, and it was postulated that the effects of Lt$\beta$R–Ig were mediated primarily by its action on T cells. Because cuprizone is not a T-cell-mediated model, our study represents the first evidence that Lt$\beta$R inhibition effects pathology other than that induced by T cells. The role of Lt$\beta$R in remyelination had not been analyzed before this study. Mice treated with Lt$\beta$R–mIg showed an increased number of GST$\pi^+$ oligodendrocytes in the corpus callosum and were able to remyelinate more efficiently as determined by LFB and MBP staining (Fig. 6*B*,*C*). Thus, by inhibiting Lt$\alpha$–Lt$\beta$R signaling, both proliferation and maturation of oligodendrocyte progenitor cells were enhanced. The mechanism of action of Lt$\beta$R–Ig is unclear but deserving of in depth analysis because it may unveil important regulatory events that lead to remyelination.

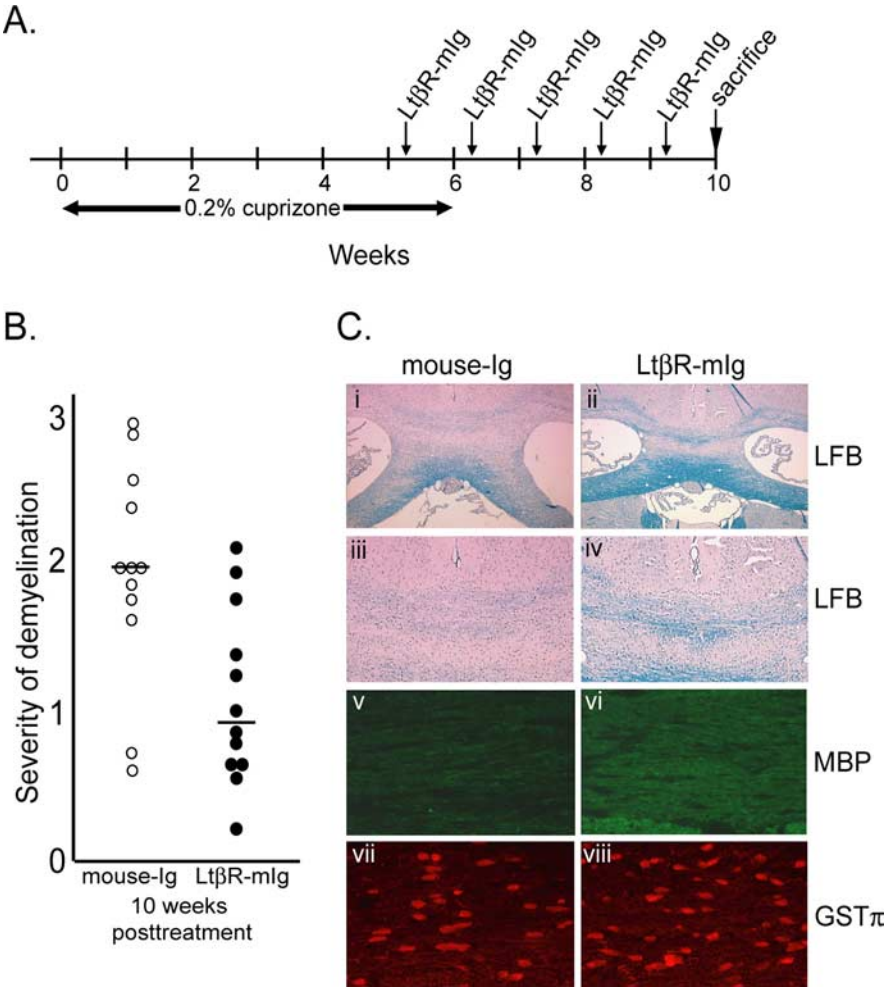


**Figure 6.** Therapeutic inhibition of Lt$\beta$R significantly enhances remyelination in a posttreatment paradigm. ***A***, C57BL/6 mice were treated with 0.2% cuprizone for 6 weeks and allowed to remyelinate for 4 weeks before they were killed. Mice received weekly injections of either Lt$\beta$R–mIg or control mouse Ig beginning 5 weeks plus 2 d after the start of cuprizone treatment (the approximate height of demyelination), as indicated by small arrows. ***B***, Remyelination was enhanced on inhibition of Lt$\beta$R signaling. LFB–PAS-stained paraffin sections were graded on a scale of 0 (normal myelination) to 3 (complete demyelination) by three double-blinded investigators. Each circle represents an individual mouse: open circles, control mouse Ig-treated mice; filled circles, Lt$\beta$R–mIg-treated mice. Horizontal lines indicate the median score of each group. Significant enhancement of remyelination was observed in Lt$\beta$R–mIg-treated mice compared with mice treated with control mouse Ig ( $p < 0.007$). ***C***, Representative LFB–PAS pictures at 10 weeks demonstrate the enhanced remyelination in Lt$\beta$R–mIg-treated mice (***ii***) compared with control mouse Ig-treated mice (***i***). High-magnification images of the corpus callosum of Lt$\beta$R–mIg-treated (***iv***) and control mouse Ig-treated (***iii***) mice demonstrate the lack of myelinated fibers and greater inflammation in control mouse Ig-treated mice during remyelination. Immunohistochemistry for MBP confirmed enhanced remyelination in Lt$\beta$R–mIg-treated mice (***vi***) compared with control mouse Ig-treated mice (***v***). Representative GST$\pi$-immunostained images of the corpus callosum demonstrating more oligodendrocytes in mice treated with Lt$\beta$R–mIg inhibitor (***viii***) than mice treated with the control mouse Ig (***vii***).

In conclusion, we hypothesize that Lt$\beta$R on glial cells, likely through direct interaction with membrane Lt$\alpha\beta$ heterotrimers on astrocytes, contribute to exacerbated demyelination and impede remyelination. This study bodes well for the use of Lt$\beta$R–Ig as a candidate biological therapy in demyelinating disorders, because inhibition has dual beneficial outcomes, both delaying demyelination and promoting remyelination. This provides a substantial rationale to explore Lt$\beta$R inhibitors for treating demyelinating disorders. The pharmacologic inhibition of TNF$\alpha$, which once was believed to be strictly proinflammatory, was detrimental to MS patients and resulted in symptom exacerbation (van Oosten et al., 1996; The Lenercept Multiple Sclerosis Study Group and The University of British Columbia MS/MRI Analysis Group, 1999; Arnett et al., 2001). Since the realization that TNF$\alpha$ has dual roles, being both detrimental during demyelination but required for oligodendrocyte progenitor proliferation and remyelination (Liu et al., 1998; Arnett et al., 2001; Kassiotis and Kollias, 2001), the results of the clinical studies are easier to interpret. In contrast, we find that inhibition of Lt$\alpha\beta$–Lt$\beta$R signaling is beneficial during both demyelination and remyelination, thus making lymphotoxin inhibitors better candi-

date biological therapies for the control of inflammatory demyelinating disorders.

## References


Arnett HA, Mason J, Marino M, Suzuki K, Matsushima GK, Ting JP (2001) TNF alpha promotes proliferation of oligodendrocyte progenitors and remyelination. Nat Neurosci 4:1116–1122.

Arnett HA, Hellendall RP, Matsushima GK, Suzuki K, Laubach VE, Sherman P, Ting JP (2002) The protective role of nitric oxide in a neurotoxicant-induced demyelinating model. J Immunol 168:427–433.

Arnett HA, Wang Y, Matsushima GK, Suzuki K, Ting JP (2003) Functional genomic analysis of remyelination reveals importance of inflammation in oligodendrocyte regeneration. J Neurosci 23:9824–9832.

Barnett MH, Prineas JW (2004) Relapsing and remitting multiple sclerosis: pathology of the newly forming lesion. Ann Neurol 55:458–468.

Baud V, Karin M (2001) Signal transduction by tumor necrosis factor and its relatives. Trends Cell Biol 11:372–377.

Chin R, Wang J, Fu YX (2003) Lymphoid microenvironment in the gut for immunoglobulin A and inflammation. Immunol Rev 195:190–201.

Crowe PD, VanArsdale TL, Walter BN, Ware CF, Hession C, Ehrenfels B, Browning JL, Din WS, Goodwin RG, Smith CA (1994) A lymphotoxin-beta-specific receptor. Science 264:707–710.

Dejardin E, Droin NM, Delhase M, Haas E, Cao Y, Makris C, Li ZW, Karin M, Ware CF, Green DR (2002) The lymphotoxin-beta receptor induces different patterns of gene expression via two NF-kappaB pathways. Immunity 17:525–535.

Dempsey PW, Doyle SE, He JQ, Cheng G (2003) The signaling adaptors and pathways activated by TNF superfamily. Cytokine Growth Factor Rev 14:193–209.

Futterer A, Mink K, Luz A, Kosco-Vilbois MH, Pfeffer K (1998) The lymphotoxin beta receptor controls organogenesis and affinity maturation in peripheral lymphoid tissues. Immunity 9:59–70.

Gommerman JL, Browning JL (2003) Lymphotoxin/light, lymphoid microenvironments and autoimmune disease. Nat Rev Immunol 3:642–655.

Gommerman JL, Giza K, Perper S, Sizing I, Ngam-Ek A, Nickerson-Nutter C, Browning JL (2003) A role for surface lymphotoxin in experimental autoimmune encephalomyelitis independent of LIGHT. J Clin Invest 112:755–767.

Granger SW, Ware CF (2001) Turning on LIGHT. J Clin Invest 108:1741–1742.

Hiremath MM, Saito Y, Knapp GW, Ting JP, Suzuki K, Matsushima GK (1998) Microglial/macrophage accumulation during cuprizone-induced demyelination in C57BL/6 mice. J Neuroimmunol 92:38–49.

Kassiotis G, Kollias G (2001) Uncoupling the proinflammatory from the immunosuppressive properties of tumor necrosis factor (TNF) at the p55 TNF receptor level: implications for pathogenesis and therapy of autoimmune demyelination. J Exp Med 193:427–434.

Korner H, Lemckert FA, Chaudhri G, Etteldorf S, Sedgwick JD (1997) Tumor necrosis factor blockade in actively induced experimental autoimmune encephalomyelitis prevents clinical disease despite activated T cell infiltration to the central nervous system. Eur J Immunol 27:1973–1981.

Lassmann H, Ransohoff RM (2004) The CD4-Th1 model for multiple sclerosis: a crucial re-appraisal. Trends Immunol 25:132–137.

Lin X, Ma X, Rodriguez M, Feng X, Zoecklein L, Fu YX, Roos RP (2003) Membrane lymphotoxin is required for resistance to Theiler's virus infection. Int Immunol 15:955–962.

Liu J, Marino MW, Wong G, Grail D, Dunn A, Bettadapura J, Slavin AJ, Old L, Bernard CC (1998) TNF is a potent anti-inflammatory cytokine in autoimmune-mediated demyelination. Nat Med 4:78–83.

Locksley RM, Killeen N, Lenardo MJ (2001) The TNF and TNF receptor superfamilies: integrating mammalian biology. Cell 104:487–501.

Lucchinetti C, Bruck W, Parisi J, Scheithauer B, Rodriguez M, Lassmann H (2000) Heterogeneity of multiple sclerosis lesions: implications for the pathogenesis of demyelination. Ann Neurol 47:707–717.

Mason JL, Jones JJ, Taniike M, Morell P, Suzuki K, Matsushima GK (2000) Mature oligodendrocyte apoptosis precedes IGF-1 production and oligodendrocyte progenitor accumulation and differentiation during demyelination/remyelination. J Neurosci Res 61:251–262.

Matsushima GK, Morell P (2001) The neurotoxicant, cuprizone, as a model to study demyelination and remyelination in the central nervous system. Brain Pathol 11:107–116.

Peterson JW, Bo L, Mork S, Chang A, Trapp BD (2001) Transected neurites, apoptotic neurons, and reduced inflammation in cortical multiple sclerosis lesions. Ann Neurol 50:389–400.

Plant S, Arnett H, Ting J (2005) Astroglial-derived lymphotoxin-alpha exacerbates inflammation and demyelination, but not remyelination. Glia 49:1–14.

Probert L, Eugster HP, Akassoglou K, Bauer J, Frei K, Lassmann H, Fontana A (2000) TNFR1 signalling is critical for the development of demyelination and the limitation of T-cell responses during immune-mediated CNS disease. Brain 123:2005–2019.

Raine CS, Bonetti B, Cannella B (1998) Multiple sclerosis: expression of molecules of the tumor necrosis factor ligand and receptor families in relationship to the demyelinated plaque. Rev Neurol (Paris) 154:577–585.

Robinson WH, Genovese MC, Moreland LW (2001) Demyelinating and neurologic events reported in association with tumor necrosis factor alpha antagonism: by what mechanisms could tumor necrosis factor alpha antagonists improve rheumatoid arthritis but exacerbate multiple sclerosis? Arthritis Rheum 44:1977–1983.

Ruddle NH, Bergman CM, McGrath KM, Lingenheld EG, Grunnet ML, Padula SJ, Clark RB (1990) An antibody to lymphotoxin and tumor necrosis factor prevents transfer of experimental allergic encephalomyelitis. J Exp Med 172:1193–1200.

Schmid CD, Sautkulis LN, Danielson PE, Cooper J, Hasel KW, Hilbush BS, Sutcliffe JG, Carson MJ (2002) Heterogeneous expression of the triggering receptor expressed on myeloid cells-2 on adult murine microglia. J Neurochem 83:1309–1320.

Sicotte NL, Voskuhl RR (2001) Onset of multiple sclerosis associated with anti-TNF therapy. Neurology 57:1885–1888.

Tansey FA, Cammer W (1991) A pi form of glutathione-S-transferase is a myelin- and oligodendrocyte-associated enzyme in mouse brain. J Neurochem 57:95–102.

The Lenercept Multiple Sclerosis Study Group and The University of British Columbia MS/MRI Analysis Group (1999) TNF neutralization in MS: results of a randomized, placebo-controlled multicenter study. Neurology 53:457–465.

van Oosten BW, Barkhof F, Truyen L, Boringa JB, Bertelsmann FW, von Blomberg BM, Woody JN, Hartung HP, Polman CH (1996) Increased MRI activity and immune activation in two multiple sclerosis patients treated with the monoclonal anti-tumor necrosis factor antibody cA2. Neurology 47:1531–1534.

Ware CF, VanArsdale TL, Crowe PD, Browning JL (1995) The ligands and receptors of the lymphotoxin system. Curr Top Microbiol Immunol 198:175–218.

Wu Q, Sun Y, Wang J, Lin X, Wang Y, Pegg LE, Futterer A, Pfeffer K, Fu YX (2001) Signal via lymphotoxin-beta R on bone marrow stromal cells is required for an early checkpoint of NK cell development. J Immunol 166:1684–1689.

Zhang G (2004) Tumor necrosis factor family ligand-receptor binding. Curr Opin Struct Biol 14:154–160.